Int. J. Electrochem. Sci., 7 **(2012)** 3155 - 3166

International Journal of
ELECTROCHEMICAL
SCIENCE
www.electrochemsci.org

Investigation of a Pt_3Sn/C Electro-Catalyst in a Direct Ethanol Fuel Cell Operating at Low Temperatures for Portable Applications

S. C. Zignani[1], *E. R. Gonzalez*[1], *V. Baglio*[2,*], *S. Siracusano*[2], *A. S. Aricò*[2]

[1] Instituto de Química de São Carlos, USP, C. P. 780, São Carlos, SP 13560-970, Brazil
[2] CNR-ITAE Institute, Via Salita S. Lucia sopra Contesse 5, 98126 S. Lucia, Messina, Italy
[*]E-mail: baglio@itae.cnr.it

Received: 30 January 2012 / *Accepted:* 6 March 2012 / *Published:* 1 April 2012

A 20% Pt_3Sn/C catalyst was prepared by reduction with formic acid and used in a direct ethanol fuel cell at low temperatures. The electro-catalytic activity of this bimetallic catalyst was compared to that of a commercial 20% Pt/C catalyst. The PtSn catalyst showed better results in the investigated temperature range (30°-70°C). Generally, Sn promotes ethanol oxidation by adsorption of OH species at considerably lower potentials compared to Pt, allowing the occurrence of a bifunctional mechanism. The bimetallic catalyst was physico-chemically characterized by X-ray diffraction (XRD) and X-ray photoelectron spectroscopy (XPS) analyses. The presence of SnO_2 in the bulk and surface of the catalyst was observed. It appears that SnO_2 can enhance the ethanol electro-oxidation activity at low potentials due to the supply of oxygen-containing species for the oxidative removal of CO and CH_3CO species adsorbed on adjacent Pt active sites.

Keywords: Pt-Sn/C, ethanol oxidation, direct ethanol fuel cells, portable application

1. INTRODUCTION

The main prerequisite of a liquid fuel for polymer electrolyte fuel cell applications is a high electrochemical reactivity at relatively low temperatures. Furthermore, the fuel should be reasonably cheap, non-toxic and largely available. At present, mainly methanol is actively investigated as an alternative to hydrogen in fuel cells [1-3]. Among other possible candidates, ethanol appears to fulfill many of the above requirements. Although the oxidation of ethanol to carbon dioxide requires the cleavage of the C-C bond, previous studies have shown interesting electrochemical reactivity at temperatures $\geq$ 80 °C [4-9]. Lamy et al. observed that the main products in the electrochemical

oxidation of ethanol were CO_2, acetaldehyde and acetic acid [5]. The occurrence of CH_3CHO and CH_3COOH causes low electrical energy yield and environmental concerns. Therefore, in order to obtain a complete oxidation of ethanol to carbon dioxide, it is important to develop highly selective catalysts and/or to increase the operation temperature to enhance the electrochemical reaction rate at the anode side [4,6,10-14]. Pt has a higher activity in the electrocatalytic oxidation of organic molecules, but this material suffers of a progressive loss of catalytic activity due to a strong adsorption of intermediate species on the surface of the electrode [15]. In order to improve the electrocatalytic activity of platinum for ethanol oxidation, platinum was often modified by adding a second metal like Ru [16-19], Ni [20], Mo [21], Sn [22-26], thus promoting the electrocatalytic activity of pure platinum. Tsiakaras showed that Sn, Ru, Pd and W can enhance ethanol electro-oxidation activity over Pt in the following order: PtSn/C>PtRu/C>PtW/C≥PtPd/C>Pt/C. Thus, Sn plays an important role in the ethanol electrooxidation and consequently improves DEFC performance [27]. The PtSn/C electrocatalyst performance also depends greatly on preparation procedures and Pt:Sn atomic ratios [28-35].

Concerning with the oxidation state of Sn that is preferable for ethanol oxidation, there is a large debate in the literature. However, most considerations are based on bulk analysis of the catalysts and, if one excludes cyclic voltammetries, in general, limited efforts have been devoted on the study of the outermost layers by surface sensitive analytical tools. The presence of Sn oxides as well as metallic tin on the catalyst surface can supply oxygen-containing species for the oxidative removal of CO and CH_3CO species adsorbed on adjacent Pt active sites, enhancing in this way the ethanol electro-oxidation activity at low potentials. Moreover, the electronic effect ascribed to a second metal on the neighbouring Pt atoms may modify the adsorption characteristic of the reacting species on the surface of bimetallic catalysts [36].

The development of direct ethanol fuel cell depends on the progress in the electrocatalytic materials for ethanol electrooxidation to a great extent. Ethanol adsorption, dissociation and oxidation are mainly affected by the composition and structure of catalysts and the catalyst preparation procedure plays a crucial role in electrocatalysts composition and structure, especially in the interaction between different components [37-40].

In this study, a Pt–Sn/C catalyst, with a nominal Pt:Sn ratio of 3:1, was prepared by the formic acid method (FAM). It was physico-chemically characterized both in terms of bulk and surface properties, and investigated in a direct ethanol fuel cell operating in the range 30-70°C for a potential application in portable electronic devices. No many attempts have been made to assess DEFC performance in the low temperature range useful for portable applications as well as in the presence of air feed at the cathode which is appropriate for practical uses.

2. EXPERIMENTAL PART

2.1 Catalyst preparation

The Pt–Sn/C electrocatalyst was prepared by the formic acid method [29], consisting in the addition of a formic acid solution on a high surface area carbon (Vulcan XC-72, Cabot, 240 $m^2 g^{-1}$).

An appropriate amount of the carbon powder substrate was suspended in 0.5M formic acid solution and the suspension was heated to 80 °C. Chloroplatinic acid ($H_2PtCl_6 \cdot 6H_2O$, Johnson Matthey) and tin chloride ($SnCl_2 \cdot 2H_2O$, MERCK) solutions were slowly added to the carbon suspension. The slurry was maintained at 80 °C for 5h. The suspension was left to cool at room temperature, and the solid was filtered, washed thoroughly with water, and finally dried in an oven at 90 °C for 2 hours. The catalysts consisted of 20% (w/w) metal (Pt + Sn) on carbon with a nominal Pt:Sn atomic ratio of 3:1.

2.2 Structural and chemical characterization

The crystalline structure of the supported catalyst was determined by using the powder X-ray diffraction (XRD) technique. An XRD pattern of the electrocatalyst was obtained by a universal diffractometer Rigaku Model Ultima IV" (Rigaku Corp., Japan) operating with Cu kα radiation (λ= 0.15406nm) generated at 40 kV and 20 mA. Scans were carried out at 2° min^{-1} for 2θ values between 15 and 100 degrees. X-ray fluorescence (XRF) analysis of the catalyst was carried out to confirm the Pt/Sn atomic ratio for the electrocatalyst and to verify the absence of impurities. The XRF analysis was made by a Bruker AXS S4 Explorer spectrometer operating at a power of 1 kW and equipped with a Rh X-ray source, a LiF 220 crystal analyzer and a 0.12 degree divergence collimator.

2.3 Surface characterization

X-ray photoelectron spectroscopy (XPS) measurements were performed by using a Physical Electronics (PHI) 5800-01 spectrometer. A monochromatic AlKa X-ray source was used at a power of 350 W. Spectra were obtained with pass energies of 58.7 eV for elemental analysis (composition) and 11.75 eV for the determination of the oxidation states. The pressure in the analysis chamber of the spectrometer was $1 \cdot 10^{-9}$ Torr during the measurements. The Ag $3d_{5/2}$ peak of an Ag foil was taken, after argon sputtering, for checking the calibration of the binding energy (BE) scale. The quantitative evaluation of each peak was obtained by dividing the integrated peak area by atomic sensitivity factors, which were calculated from the ionization cross-sections, the mean free electron escape depth and the measured transmission functions of the spectrometer. XPS data have been interpreted by using the on-line library of oxidation states implemented in the PHI MULTIPAK 6.1 software and the PHI Handbook of X-ray photoelectron spectroscopy [41].

2.4 Eletrochemical studies

All experiments were conducted with a Fuel Cell Technologies, Inc. test station. In order to test the electrochemical behaviour in a single DEFC fed with ethanol and oxygen or air, the electrodes were composed of diffusion and catalytic layers [42].

The electrocatalyst was applied on the diffusion layer (E-TEK), in the form of an homogeneous dispersion of Pt–Sn/C, 33wt.% Nafion solution (5 wt. %, Aldrich) and isopropanol (Merck). A 30 % Pt/C (E-TEK) was used at the cathode. The electrodes contained 2 mg Pt cm^{-2} at the anode and 2 mg Pt

cm^{-2} at the cathode. These were hot pressed onto a Nafion 117 membrane and installed into a single cell test fixture [43]. A commercial 20% Pt/C E-TEK catalyst was also investigated at the anode for comparison.

3. RESULTS AND DISCUSSION

3.1 Structural analysis

Table 1 reports the bulk composition of the catalyst as determined by XRF analysis and the nominal one calculated from the amount of precursors used in the preparation of the catalyst. Structural characteristics of the catalyst are also reported in Table 1 and compared to the commercial catalyst.

Table 1. Composition and physico-chemical characteristics of the in-house prepared Pt_3Sn/C catalyst and a commercial Pt/C (E-TEK) catalyst.

Nominal Composition	Bulk Composition (XRF)	Lattice Parameter nm	Crystallite Size (XRD) nm	Degree of Alloying %
20% Pt/C (E-TEK)	-	0.3928	3.0	-
20%Pt_3Sn_1/C (FAM)	$Pt_{73}Sn_{27}/C$	0.3943	3.6	7.0

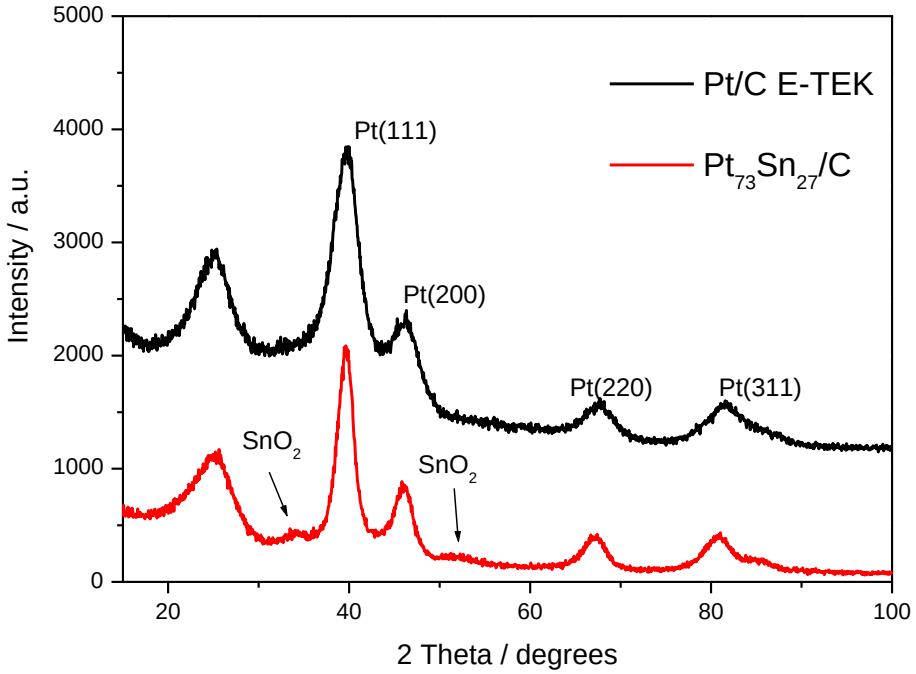

Figure 1. X-ray patterns of the in-house Pt_3Sn/C and Pt/C (E-TEK) catalysts.

A reasonable agreement between the nominal composition and the effective bulk composition determined by XRF is observed. The presence of other species (impurities) was not detected.

Figure 1 shows the X-ray diffraction pattern for the catalyst $Pt_{73}Sn_{27}/C$ prepared with formic acid compared to the commercial 20% Pt/C. The XRD patterns show the characteristic peaks of the face-centered cubic (fcc) crystalline structure associated to platinum. The metal crystallite size, calculated from the (220) reflection of Pt according to Scherrer formula, and lattice parameters are listed in Table 1.

The lattice parameter of the Pt_3Sn/C catalyst prepared by reduction with formic acid was slightly larger than that of the commercial Pt/C catalyst, i.e. 0.3943 nm for Pt_3Sn/C compared to 0.3928 nm for Pt/C, as revealed by the shift of Pt (220) peak to lower Bragg angles. The larger lattice parameter indicates that there is an incorporation of Sn atoms into the lattice of Pt. A clear evidence of SnO_2 in the X-ray pattern of Pt_3Sn/C is observed in Figure 1. Probably, this is the cause of the reduced degree of alloying (see Table 1).

3.2 Surface analysis

Figure 2 shows the XPS survey analysis of the Pt_3Sn/C catalyst. The atomic Pt/Sn ratio on the surface shows a surface composition slightly different from the nominal composition. In fact, the relative tin content on the surface is larger than in the bulk indicating a clear enrichment of Sn in the outermost layers.

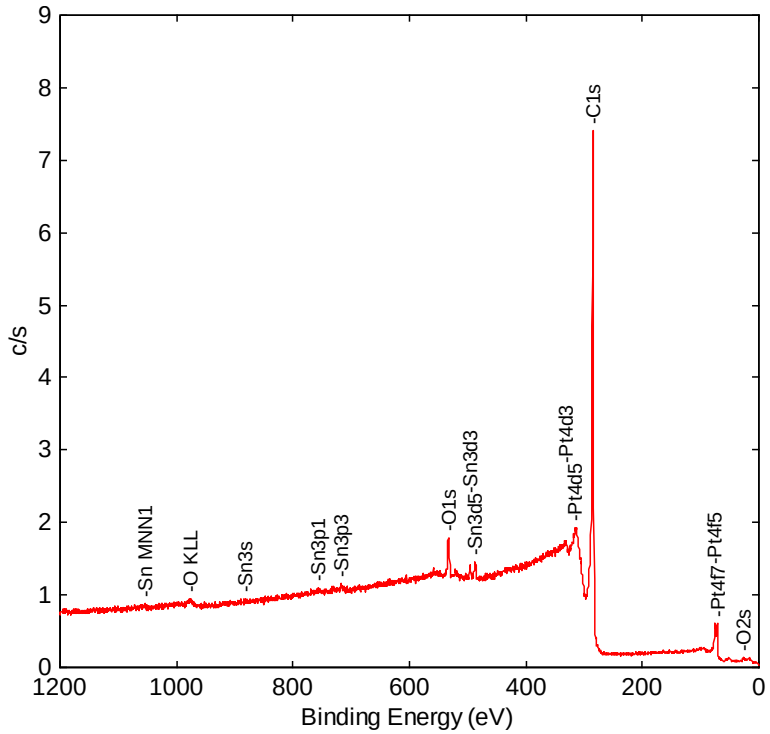

Figure 2. XPS survey analysis of the Pt_3Sn/C catalyst.

This could be explained in terms of the different kinetics of the reduction process of the platinum and tin. As previously mentioned, platinum is more easily reduced than tin, leading to a Pt-enriched core, and hence, a Sn-enriched shell particle.

XPS spectrum of the Pt_3Sn/C catalyst (Figure 3) shows that Pt is mainly metallic in the sample (B.E. 71.4 eV for Pt $4f_{7/2}$ and 74.7 eV for Pt $4f_{5/2}$), whereas tin is mainly oxidized on the surface (B.E. 487.6 eV for Sn $3d_{5/2}$ and 495.9 eV for $3d_{3/2}$) denoting the prevailing occurrence of Sn^{4+} in the outermost layers of the catalyst nanoparticles. However, a proper fraction of metallic tin is also observed (485.5 eV for Sn $3d_{5/2}$ and 494.3 eV for $3d_{3/2}$).

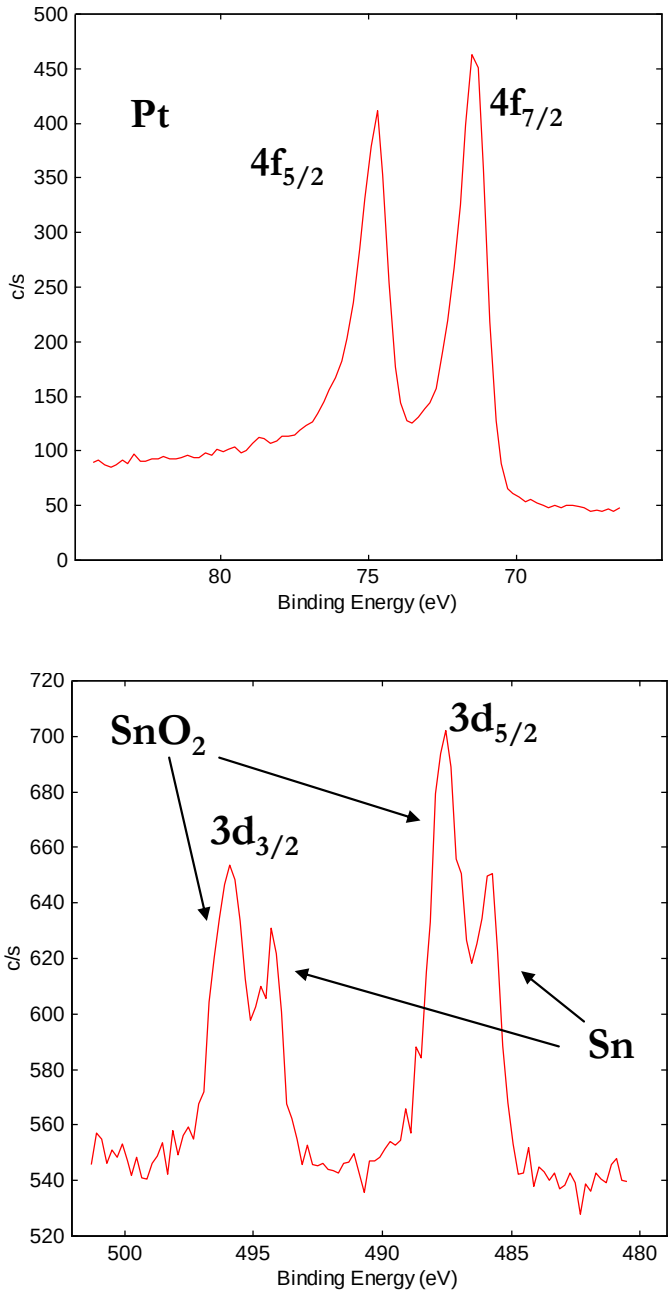

Figure 3. XPS spectrum of Pt 4f and Sn 3d lines for the Pt_3Sn/C catalyst.

3.4 Electrochemical Measurements

3.4.1. Polarization curves

The results obtained in the direct ethanol fuel cell in terms of polarization and power density curves for Pt_3Sn/C-based MEA operating in a temperature range from 30°C to 70°C under oxygen and air feed are shown in Figures 4 and 5, respectively.

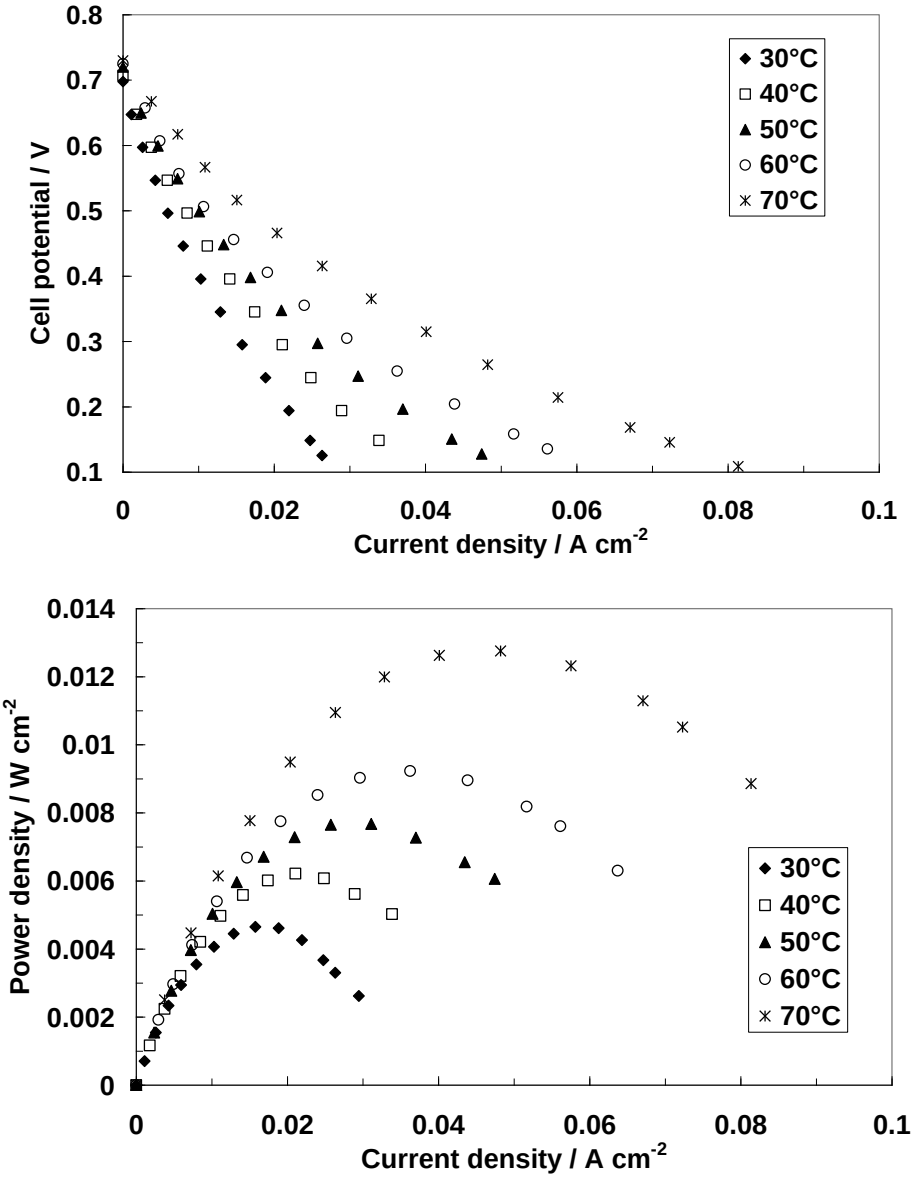

Figure 4. Polarization (a) and power density (b) curves for the Pt_3Sn/C catalyst at different temperatures under oxygen feed.

As expected, a higher performance was recorded at higher temperatures due to the increase of reaction kinetics for ethanol oxidation with temperature. The power density increased from 5 mW cm^{-2}

up to 13 mW cm^{-2} passing from 30°C to 70°C. The modest performance is attributable mainly to the slow ethanol oxidation reaction rate at these temperatures and a possible poisoning effect of the cathode due to the ethanol cross-over. It is pointed out that a moderate Pt content (2 mg cm^{-2}) was used in both electrodes in the present investigation in order to evaluate the catalysts under viable conditions. Moreover, in order to assess the catalysts under practical conditions, same polarization measurements were carried out feeding air at the cathode (Figure 5). Under these conditions, a decrease of performance of about 30-35% was recorded compared to oxygen feed; whereas, the open circuit voltage (OCV) decreased of about 100 mV passing from oxygen to air. The latter effect appears to be related to the increase of cathode poisoning by the ethanol cross-over in the presence of air compared to O_2 feed. Pure Oxygen allows a faster oxidation of adsorbed ethanolic residues.

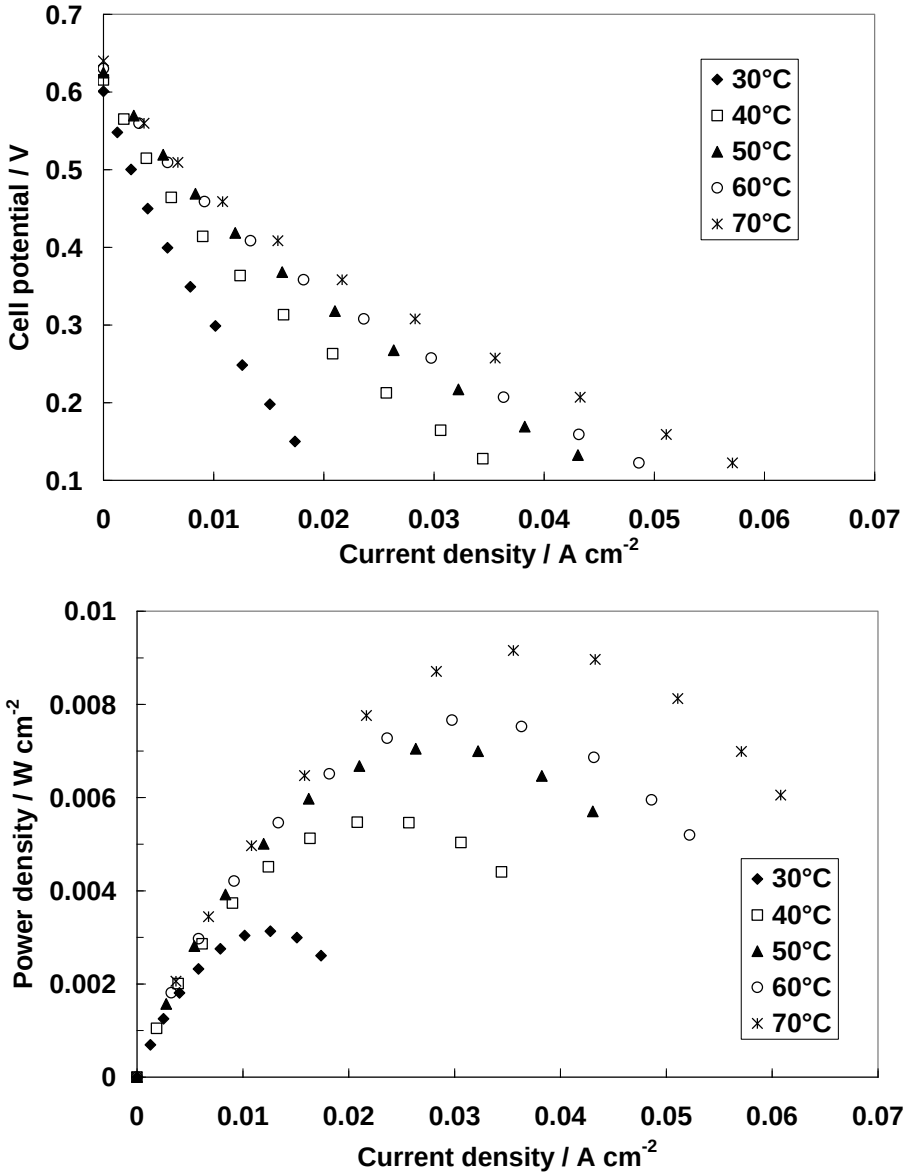

Figure 5. Polarization (a) and power density (b) curves for the Pt_3Sn/C catalyst at different temperatures under air feed.

To confirm the beneficial effect of Sn in enhancing the catalytic activity of Pt towards ethanol electro-oxidation in particular at low temperatures, a 20% Pt/C E-TEK was investigated at the anode in a direct ethanol fuel cell under the same conditions of the previous experiments using 20% Pt_3Sn/C. A comparison at 30°C between Pt and PtSn anodic-catalyst-based cells is reported in Figure 6. When Pt_3Sn/C was used as the anode catalyst, the single cell at 30°C showed a higher performance, in particular in the activation region. The OCV was larger for PtSn-based cell, whereas at higher current density, due to a lower cell resistance, the Pt-based cell showed similar characteristics.

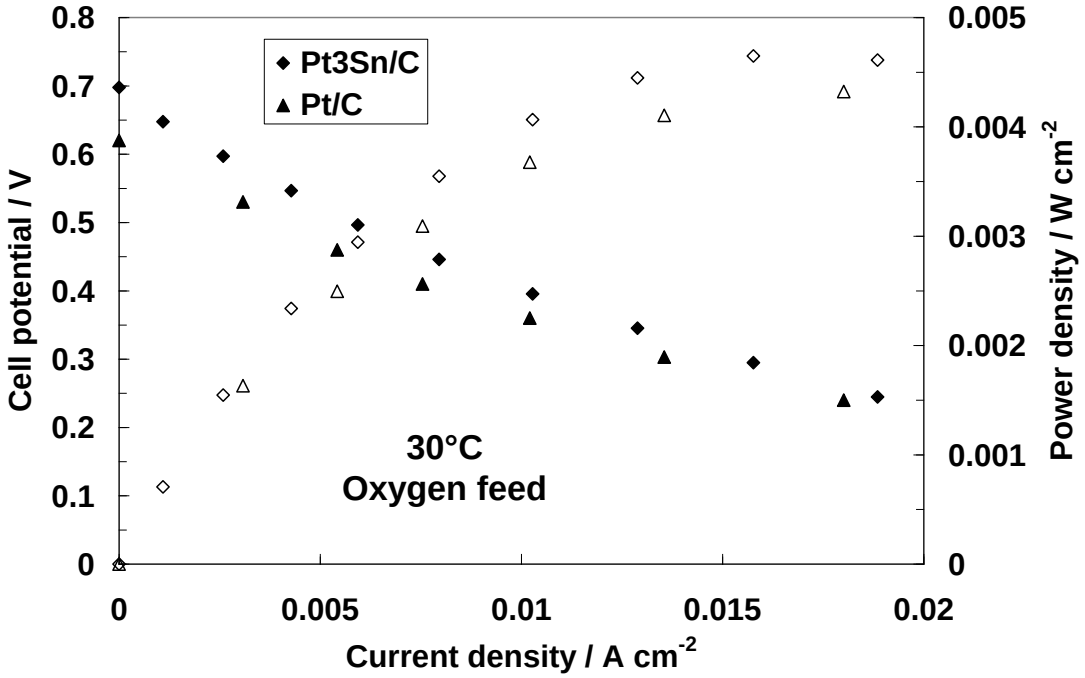

Figure 6. Comparison of polarization and power density curves obtained with Pt_3Sn/C and Pt/C (E-TEK) anode catalysts at 30°C and oxygen feed.

It was reported that the addition of transition metals, such as Sn, to Pt based catalysts promotes ethanol oxidation by adsorption of OH species at considerably lower potentials compared to Pt, allowing the occurrence of a bifunctional mechanism [5,16,17]. Moreover, the electronic effect caused by a second metal on the neighbouring Pt atoms may lead to a weakening of adsorbed species in the bimetallic catalyst [36]. Delime et al. [28] prepared bimetallic non-alloyed Pt–Sn catalysts and observed that the presence of tin leads to an increase of current density for the electro-oxidation of ethanol, with an optimum Sn content of 20 at%. Lamy et al. [8] studied in half-cell experiments the electro-oxidation of ethanol on Pt–Sn catalysts at room temperature. A large enhancement of electrocatalytic activity was observed for non-alloyed Pt–Sn with 10 at.% Sn. However, limited attention was devoted to the investigation of PtSn/C catalysts in a fuel cell under practical conditions for portable applications, i.e. low temperature and low Pt loading (also in conjunction with the use of air as the oxidant). At 70°C the trend in the electrochemical behaviour of Pt- and PtSn-based cells is similar to that reported at 30°C (Figure 7). At high current density the Pt/C-based cell performs

comparally to the PtSn/C catalyst-based DEFC probably due to the fact that the presence of SnO_2 in the bimetallic catalyst produces a higher cell resistance.

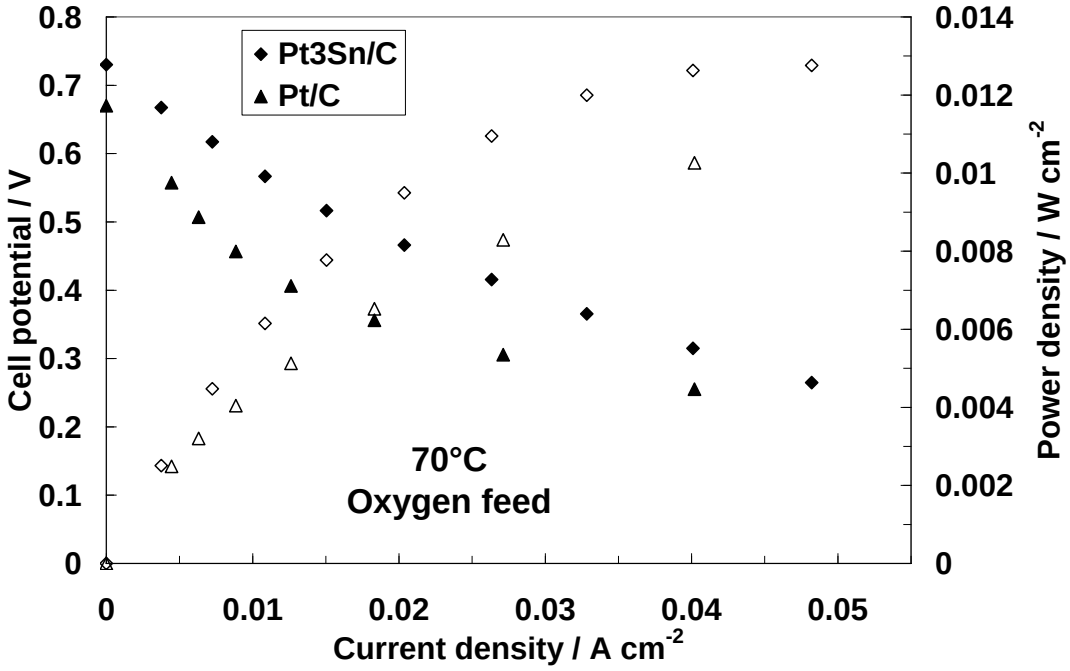

Figure 7. Comparison of polarization and power density curves obtained with Pt_3Sn/C and Pt/C (E-TEK) anode catalysts at 70°C and oxygen feed.

5. CONCLUSIONS

A 20% Pt_3Sn/C catalyst was prepared by reduction with formic acid and used in a direct ethanol fuel cell at low temperatures. Such a composition was selected to provide an optimum balance between the amount of tin and platinum present on the surface, and to promote electronic and structural effects. The amount of tin oxides should be sufficient to provide –OH groups without decreasing excessively the conductivity of the catalytic layer due to the occurrence of SnO_2. This bimetallic catalyst was compared to a commercial 20% Pt/C catalyst showing better results in the investigated temperature range. However, the performance of the PtSn-based cell appears at the moment not sufficiently high for a practical application of direct ethanol fuel cells in portable electronic devices.

ACKNOWLEDGEMENTS

The authors of Instituto de Química de São Carlos gratefully acknowledge the financial support of the Conselho Nacional de Desenvolvimento Científico e Tecnológico (CNPq), Coordenação de Aperfeiçoamento de Pessoal de Nível Superior (CAPES). S.C. Zignani acknowledges the assistance of CNR-ITAE during her 1-year stay.

References

1. A.S. Aricò, V. Baglio, V. Antonucci, Direct Methanol Fuel Cells: History, Status and Perspectives, in *Electrocatalysis of Direct Methanol Fuel Cells*. Eds. H. Liu and J. Zhang; WILEY-VCH (2009) 1-78.
2. V. Baglio, A. Di Blasi, E. Modica, P. Cretì, V. Antonucci and A.S. Aricò, *Int. J. Electrochem. Sci.*, 1 (2006) 71.
3. H. Liu, C. Song, L. Zhang, J. Zhang, H. Wang and D. P. Wilkinson, *J. Power Sources*, 155 (2006) 95.
4. A. S. Aricò, P. Creti, P. L. Antonucci and V. Antonucci, *Electrochem. Solid-State Lett.*, 1 (1998) 66.
5. S. Rousseau, C. Coutanceau, C. Lamy and J.M. Léger, *J. Power Sources*, 158 (2006) 18.
6. A. Di Blasi, V. Baglio, A. Stassi, C. D'Urso, V. Antonucci and A. S. Aricò, *ECS Transactions*, 3 (1) (2006) 1317.
7. W.J. Zhou, S.Q. Song, W.Z. Li, Z.H. Zhou, G.Q. Sun, Q. Xin, S. Douvartzides and P. Tsiakaras, *J. Power Sources*, 140 (2005) 50.
8. C. Lamy, S. Rousseau, E.M. Belgsir, C. Coutanceau and J.M. Leger, *Electrochim. Acta*, 49 (2004) 3901.
9. Z. Liu, X.Y. Ling, X. Su, J.Y. Lee and L.M. Gan, *J. Power Sources*, 149 (2005) 1.
10. S. Song and P. Tsiakaras, *Applied Catalysis B: Environmental*, 63 (2006) 187.
11. M. Brandalise, M. M. Tusi, R. M. S. Rodrigues, E. V. Spinacé and A. O. Neto, *Int. J. Electrochem. Sci.*, 5 (2010) 1879.
12. F. Wang, Y. Zheng and Y. Guo, *Fuel Cells*, 10 (2010) 1100.
13. R.F.B. De Souza, L.S. Parreira, J.C.M. Silva, F.C. Simoes, M.L. Calegaro , M.J. Giz, G.A. Camara, A.O. Neto and M.C. Santos, *Int. J. Hydrogen Energy*, 36 (2011) 11519.
14. H. Li, D. Kang, H. Wang and R. Wang, *Int. J. Electrochem. Sci*., 6 (2011) 1058.
15. E. Antolini, *J. Power Sources*, 170 (2007) 1.
16. W. Zhou,W. Li, S. Song, Z. Zhou, L. Jiang, G. Sun, Q. Xin, K. Poulianitis, S. Kontou and P. Tsiakaras, *J. Power Sources*, 131 (2004) 217.
17. H. Wang, Z. Jusys and R. Behm, *J. Power Sources*, 154 (2006) 351.
18. A. O. Neto, R. W. R. Verjulio-Silva, M. Linardi and E.V. Spinacé, *Int. J. Electrochem. Sci.*, 4 (2009) 954.
19. G. Camara, R. Lima and T. Iwasita, *Electrochem. Commun*., 6 (2004) 812.
20. E. Spinacé, M. Linardi, A. Neto, *Electrochem. Commun*., 7 (2005) 365.
21. A. Neto, M. Giz, J. Perez, E. Ticianelli and E. Gonzalez, *J. Electrochem. Soc.*, 149 (2002) A272.
22. F. Colmati, E. Antolini and E. Gonzalez, *Appl. Catal. B: Environ*., 73 (2007) 106.
23. L. Jiang, G. Sun, Z. Zhou, W. Zhou and Q. Xin, *Catal. Today*, 93 (2004) 665.
24. F. Vigier, C. Coutanceau, F. Hahn, E. Belgsir and C. Lamy, *J. Electroanal. Chem*., 563 (2004) 81.
25. E. Antolini and E. R. Gonzalez, *Electrochimica Acta*, 55 (2010) 6485.
26. W. Zhou, Z. Zhou, S. Song, W. Li, G. Sun, P. Tsiakaras and Q. Xin, *Appl. Catal. B: Environ.*, 46 (2003) 273–285.
27. P.E. Tsiakaras, *J. Power Sources*, 171 (2007) 1.
28. F. Delime, J.-M. Léger and C. Lamy, *J. Appl. Electrochem*., 29 (1999) 1249.
29. E.R. Gonzalez, E.A. Ticianelli, A.I.N. Pinheiro and J. Perez, *Brazilian Patent*, INPI-SP no. 00321 (1997)
30. E. Antolini and E.R. González, *Catal. Today*, 160 (2011) 28.
31. J. Lobato, P. Cañizares, M.A. Rodrigo and J.J. Linares, *Appl. Catal. B: Environ.*, 91 (2009) 269.
32. J. Lobato, P. Cañizares, D. Úbeda, F.J. Pinar and M.A. Rodrigo, *Appl. Catal. B: Environ.*, 106 (2011) 174.

33. J. Barroso, A.R. Pierna, T.C. Blanco, E. Morallón and F. Huerta, *Int. J. Hydrogen Energy*, 36 (2011) 12574.
34. J. Barroso, A.R. Pierna, T.C. Blanco, E. Morallón and F. Huerta, *J. Power Sources*, 196 (2011) 4193.
35. A. Bonesi, G. Garaventa, W.E. Triaca and A.M. Castro Luna, *Int. J. Hydrogen Energy*, 33 (2008) 3499.
36. P. Liu, A. Logadottir and J.K. Nørskov, *Electrochim. Acta*, 48 (2003) 3731.
37. M. Zhu, G. Sun and Q. Xin, *Electrochim. Acta*, 54 (2009) 1511.
38. H. Li, D. Kang, H. Wang and R. Wang, *Int. J. Electrochem. Sci.*, 6 (2011) 1058.
39. J. Parrondo, R. Santhanam, F. Mijangos and B. Rambabu, *Int. J. Electrochem. Sci*., 5 (2010) 1342.
40. M. Brandalise, M.M. Tusi, R.M. Piasentin, M. Linardi, E.V. Spinacé and A. O. Neto, *Int. J. Electrochem. Sci*., 5 (2010) 39.
41. J.F. Moulder, W.F. Stickle, P.E. Sobol and K.D. Bomben, *Handbook of X-ray Photoelectron Spectroscopy*, Physical Electronics, Inc, Eden Prairie, MN, (1995).
42. A. M. Castro Luna, A. Bonesi, W. E. Triaca, A. Di Blasi, A. Stassi, V. Baglio, V. Antonucci and A. S. Aricò, *J. Nanopart. Res*., 12 (2010) 357.
43. V. Baglio, A. Di Blasi, A.S. Aricò, V. Antonucci, P.L. Antonucci, F. Nannetti and V. Tricoli, *Electrochim. Acta*, 50 (2005) 5181.